ChemComm



COMMUNICATION

View Article Online



Cite this: Chem. Commun., 2021, **57**, 4898

Received 20th February 2021, Accepted 9th April 2021

DOI: 10.1039/d1cc00966d

rsc.li/chemcomm

One-pot synthesis of Na⁺-free Cu-SSZ-13 and its application in the NH3-SCR reaction†

Juan Wang, ab Linying Wang, b Dali Zhu, bc Wenhao Cui, bc Peng Tian*b and Zhongmin Liu ** **

Na⁺-free Cu-SSZ-13 zeolites have been rationally synthesized via a cooperative strategy, which has the advantages of rapid crystallization (9-48 h), high yield (86-94%) and adjustable Cu content. The NH₃-SCR catalytic performance and hydrothermal stability of the calcined materials were studied and correlated with their physicochemical properties.

Metal-containing zeolites are an important class of catalytic materials, and have attracted great attention in recent years due to their remarkable performance for many reactions, ^{1,2} such as hydrogenation, dehydrogenation, oxidation, etc. The micropores and cavities of zeolites can provide a confinement effect for metal species to inhibit their migration and aggregation. Meanwhile, the abundant and interconnected channels in zeolites allow free access of reactant molecules to the encapsulated metal species. On the other hand, owing to the proximity of the metal species and acid sites in the confined spaces of zeolites, cooperative bifunctional catalysts can be created, which have found wide applications.

Cu-containing SSZ-13 (CHA topology with 8-ring channels and nanosized cavities) is one of the important metalcontaining zeolites, which shows promising performance for the direct conversion of methane into methanol3,4 and has been used commercially for the NH₃-SCR reaction.⁵ NH₃-SCR technology is currently recognized as one of the most effective ways to remove environmentally harmful NO_r emissions from diesel vehicles. It has been demonstrated that the Cu-SSZ-13 SCR catalyst works in a bifunctional manner, wherein isolated Cu2+ ions act as SCR active centers, and acid sites are an NH3 reservoir that supplies NH₃ via migration for active centers.^{6,7}

In 2011, Xiao et al. 13 first reported the direct synthesis of Cu-SSZ-13 in the presence of the Cu²⁺-tetraethylenepentamine(Cu-TEPA) complex and NaOH, wherein Cu-TEPA acts as both Cu source and organic structure directing agent (OSDA). However, the Si/Al ratios of the products are low (4-7), and the Cu content is rather high. Although post-synthesis ion exchange can help remove part of Cu²⁺ and Na⁺, the hydrothermal stability of the products still needs to be improved. Subsequently, Corma et al. 14 prepared Cu-SSZ-13 following the co-template method with the use of N,N,N-trimethyl-1-adamant ammonium hydroxide (TMAdaOH) and Cu-TEPA in alkaline media (NaOH). The introduction of TMAdaOH (typical OSDA for SSZ-13) allows the control of product Cu content and Si/Al ratio at a satisfying level. Unfortunately, the synthesis period of this method is rather long (14 days). Therefore, developing a novel/one-pot strategy for the efficient synthesis of Cu-SSZ-13 with high SCR activity and hydrothermal stability would be highly desirable. Ideally, the synthesis system should not contain alkali cations (Na⁺) and yield Na⁺-free Cu-SSZ-13 product, which allows the direct conversion of the material to active catalyst with abundant acid sites by simple calcination.

Herein, we report the one-pot synthesis of Na⁺-free Cu-SSZ-13 by a designed cooperative strategy, which involves the use of TMAdaOH, Cu-amine complex, small size amine and SSZ-13 seeds. The substitution of small size amine for NaOH enables the building-up of the Na⁺-free synthetic system and can help reduce the consumption of expensive TMAdaOH. The resultant products were characterized in detail. Moreover, the NH3-SCR

Over the past few decades, great efforts have been dedicated to the synthesis and optimization of SSZ-13, including variations of organic template, Si/Al ratio, crystal morphology, etc. 8-10 Cu-SSZ-13 is generally prepared by the post-synthesis ion exchange method, 11,12 which involves multiple steps including the synthesis of SSZ-13, calcination to remove organics, NH₄⁺ ion exchange to remove Na+, Cu2+ ion exchange and finally hightemperature calcination and activation treatment. Such a complex procedure is obviously time and cost-consuming and unfavourable for industrial production.

^a Zhang Dayu School of Chemistry, Dalian University of Technology, Dalian 116024, China. E-mail: liuzm@dicp.ac.cn

^b National Engineering Laboratory for Methanol to Olefins, Dalian Institute of Chemical Physics, Chinese Academy of Sciences, Dalian 116023, China. E-mail: tianpeng@dicp.ac.cn

^c University of Chinese Academy of Sciences, Beijing 100049, China

[†] Electronic supplementary information (ESI) available: Synthesis procedures, characterizations, and catalytic reactivity test. See DOI: 10.1039/d1cc00966d

Communication ChemComm

 $\textbf{Table 1} \quad \textbf{Starting gel compositions, product phases, } \textbf{SiO}_2/\textbf{Al}_2\textbf{O}_3 \text{ ratios, } \textbf{Cu contents and yields of Na}^+ - \textbf{free } \textbf{SSZ-13} \text{ and } \textbf{CuSSZ-13} \textbf{CuSSZ-13}$

Sample ^a	x	TMAdaOH/Si O_2 in gel	Crystallization time (h)	Product phase	${ m SiO_2/Al_2O_3}$	Cu (wt%)	Cu incorporation b	Yield ^c (wt%)
SSZ-13 _{TMAOH}	_	0.05	9	CHA	24.8	_	_	86
$SSZ-13_{BA}$	_	0.05	72	CHA	24.8	_	_	87
CuSSZ-13-1	0.6	0.05	48	CHA	27.4	1.48	80%	86
CuSSZ-13-2	1.0	0.05	48	CHA	24.5	2.42	76%	90
CuSSZ-13-3	1.5	0.05	48	Amor. + CHA	_	_	_	_
CuSSZ-13-4	1.0	0.075	9	CHA	23.8	2.43	76%	93
CuSSZ-13-5	1.5	0.075	9	CHA	24.9	3.80	79%	94

^a Gel molar composition for SSZ-13_{TMAOH} and SSZ-13_{BA}: 30SiO₂: 1Al₂O₃: 3TMAOH (or 4BA): 600H₂O: 1.5TMAdaOH; gel molar composition for CuSSZ-13: 30SiO₂: 1Al₂O₃: 3TMAOH: 600H₂O: 2.25TMAdaOH: x Cu-TEPA (10 wt% seeds addition). T = 175 °C. b Cu incorporation = (Cu/Si)_{product}/ (Cu/Si)_{gel}. ^c Solid yield was calculated on the basis of inorganic oxides.

catalytic performance and hydrothermal stability of the calcined Na⁺-free Cu-SSZ-13 were investigated and correlated with its physicochemical properties.

The synthesis of Na⁺-free SSZ-13 was first explored to learn the possibility of small size amines in place of NaOH and to determine the optimal choice of amines. Table 1 lists the optimized synthesis conditions and the product compositions. Clearly, Na⁺-free SSZ-13 can be successfully synthesized under the presence of tetramethylammonium hydroxide (TMAOH) within a short crystallization time of 9 h. The usage of TMAdaOH (TMAdaOH/SiO₂ = 0.05) is at a very low value, as compared with previous works.⁸⁻¹⁰ It is noted that the appearance of seeds in the synthetic system is also very critical for the fast completion of the crystallization (Fig. S1, ESI†). Otherwise, an amorphous product was obtained even after 3 days. Besides TMAOH, many small alkylamines and NH₃ (aq) were also found to be effective for the synthesis (Table S1, ESI†). The former includes butylamine (BA), diethylamine (DEA), ethylenediamine (EDA), and piprazine hexahydrate (PIP). However, longer crystallization time was needed for alkylamines and NH3 (aq) than for TMAOH, which is likely due to their weaker alkalinity.

Fig. 1 and Fig. S2-S4 (ESI†) display the characterization results of Na⁺-free SSZ-13. The samples present typical XRD

diffraction peaks associated with the CHA-type zeolite. The SEM images reveal the cubic-like morphology of the samples with a crystal size of about 1 µm. To figure out the exact effect of small amines in the synthesis, liquid ¹³C NMR spectra of the assynthesized samples dissolved in HF solution were measured. As seen in the spectra shown in Fig. 1 and Fig. S3 (ESI†), the observed resonances are mainly associated with TMAda+ for all samples, implying that small size amines are not occluded in the products. It is thus speculated that the small size amines do not play the structure-directing role for the formation of SSZ-13 under the present conditions. They are responsible for the enhancement of gel alkalinity. This also explains well the diversity of small amines effective for the synthesis. The thermal analysis result of SSZ-13_{TMAOH} is shown in Fig. 2. The minor weight loss between 100-250 °C resulted from water desorption; the distinct weight loss between 400-750 °C was due to the removal of organics. Based on the TG and XRF results, the occluded TMAda⁺ per cage is calculated to be 1, which agrees with the value reported previously.

According to the above results, the gel system of SSZ-13_{TMAOH} with the fastest crystallization rate was employed for the synthesis exploration of Na+free CuSSZ-13. The Cu-TEPA complex was utilized as a Cu source. As shown in Table 1,

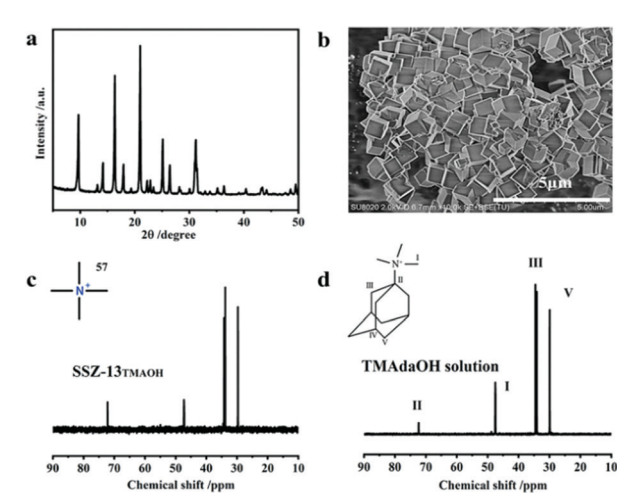


Fig. 1 (a) XRD pattern, (b) SEM image of the as-synthesized Na⁺-free SSZ-13_{TMAOH}, (c) liquid ¹³C NMR spectrum of the as-synthesized SSZ-13_{TMAOH} dissolved in HF solution and (d) liquid ¹³C NMR spectrum of TMAdaOH solution.

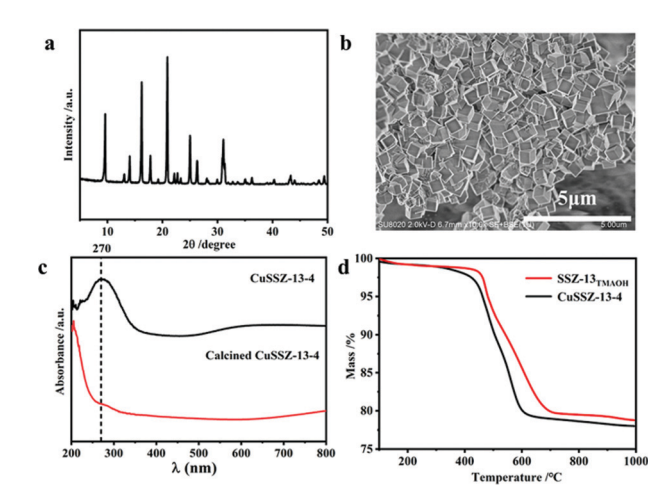


Fig. 2 (a) XRD pattern, (b) SEM image, (c) UV/Vis spectrum and (d) TG curve of the as-synthesized Na⁺-free CuSSZ-13-4. For comparison, the UV/Vis spectrum of calcined CuSSZ-13-4 and TG curve of SSZ-13_{TMAOH} are shown in (c) and (d), respectively.

ChemComm Communication

Na⁺-free CuSSZ-13 could be synthesized from the Cu-TEPAadded system of SSZ- 13_{TMAOH} , but the crystallization time had to be prolonged to 48 h to achieve well-crystallized products (CuSSZ-13-1 and CuSSZ-13-2). When the Cu/Si ratio in the starting gel was higher than 1/30, the product would be contaminated with a large amount of amorphous materials, indicating that the addition of the Cu-TEPA complex raised the difficulty of crystallization. Attempts to slightly increase the amount of TMAdaOH in the gel (OSDA/SiO2 = 0.075) can effectively speed-up the crystallization even with larger addition of the Cu source, and the syntheses completed in 9 h giving a very high yield of >90% (samples CuSSZ-13-4 and CuSSZ-13-5). The Cu incorporation degree is also calculated and listed in Table 1, showing that all samples have high Cu incorporation of above 75%.

The XRD patterns and SEM images of the as-synthesized Na⁺-free CuSSZ-13 are displayed in Fig. 2 and Fig. S5, S6 (ESI†). All samples present a typical XRD pattern of CHA-type zeolite with a crystal size of about 1 μm, similar to those of Na⁺-free SSZ-13. The UV/Vis spectra of the samples are shown in Fig. 2c and Fig. S7 (ESI†). The as-synthesized CuSSZ-13 samples present a strong absorption centered at 270 nm, which disappears in the spectra of the calcined samples. According to the previous literature, 13 this signal can be assigned to the Cu-amine complex and is a clear indication that Cu-TEPA has been incorporated into the product. Fig. 2d presents the TG result of the Na⁺-free sample. As compared with SSZ-13_{TMAOH}, CuSSZ-13-4 shows comparable organics content, but the complete removal of organics occurs at a lower temperature. This difference may imply that the decomposition of the Cu-TEPA complex is relatively easy. The textural properties of CuSSZ-13-4 were investigated by N₂ adsorption. As shown in Table S2 (ESI†), the micropore area and micropore volume are 583 m² g⁻¹ and 0.27 cm³ g⁻¹, respectively. These values are close to the results previously reported for SSZ-13 and confirm the good crystallinity of Na+-free CuSSZ-13.

The ²⁹Si and ²⁷Al MAS NMR spectra of the as-synthesized CuSSZ-13-4 are given in Fig. S8 (ESI†). The three resonances assigned at -101, -106 and -111 ppm in the ²⁹Si spectrum can be attributed to Si(3Si)(OH), Si(1Al) and Si(0Al), respectively. 15 The framework SAR is thus calculated to be 24.4, which is close to the value derived from XRF. For the ²⁷Al spectrum, the strong signal at 56 ppm is attributed to tetrahedrally coordinated framework Al species. The small peak at 5 ppm is likely to be associated with the framework octahedral Al species formed by the additional interaction with water.

CuSSZ-13-4 with a Cu/Al molar ratio of 0.31 (ion exchange level \sim 62%) was selected for the NH₃-SCR test, as previous works have suggested that this level is an optimum value to provide more active Cu²⁺ ions for the reaction and prevent the formation of large CuO_x clusters. 16 The latter would be detrimental to the long-term stability of the catalyst. 17 As shown in Fig. 3, the NO_x conversion on the fresh sample can reach \sim 100% in a wide temperature range of 200–450 °C. Upon hydrothermal aging at 750 °C for 16 h, the sample exhibits an obviously enhanced low-temperature activity (<200 °C), and almost 100% NOx conversion in the temperature range of

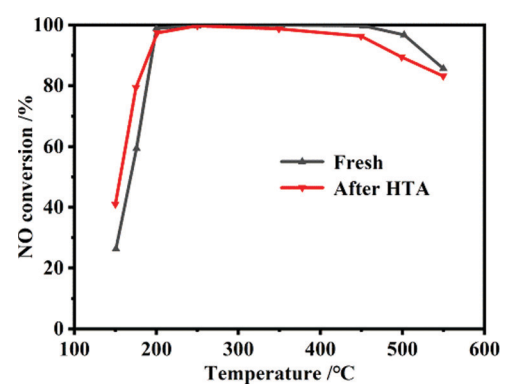


Fig. 3 Standard SCR reactions over the CuSSZ-13-4 before and after hydrothermal aging treatment (HTA). Reaction conditions: feed gas consisted of 500 ppm NH₃, 500 ppm NO, 6.4% H₂O, 6.4% O₂, balance N₂; GHSV = $100000 h^{-1}$.

200-350 °C. Although the high-temperature activity (>450 °C) over the aged sample shows a slight decline, the NO_x conversion can still be kept at higher than 80% at 550 $^{\circ}$ C. The N_2 selectivity on the catalysts is given in Fig. S9 (ESI†), which is very high (>97%) even after aging treatment.

To understand the activity variation of CuSSZ-13 before and after hydrothermal treatment, the crystallinity, acidity, reducibility and active Cu²⁺ contents of the catalysts were examined. The XRD patterns of the fresh and aged catalysts are shown in Fig. S10 (ESI†), which confirms the good structural stability of CuSSZ-13 and no peaks related to CuO species can be observed. NH₃-TPD was carried out to investigate the acid properties of the samples and the results are shown in Fig. S11 (ESI†). For SSZ-13, the strong peaks at 200 °C and 521 °C can be assigned to weakly bound NH3 and the NH3 desorbed from strong Brønsted acid sites, respectively. 18 In the case of CuSSZ-13-4, the NH₃-TPD profile shows the presence of two extra desorption peaks at 369 °C and 433 °C, which suggests that the presence of Cu species generates additional adsorption sites for NH3. Meanwhile, the high-temperature peak indicates broadening and decrease in intensity, implying the increase in heterogeneity of these sites with reduced numbers after the incorporation of Cu species. After hydrothermal aging, the high-temperature peak almost disappears, corresponding to the loss of strong Brønsted acid sites (framework dealumination). The signal around 280 °C becomes obviously enhanced, owing to the formation of Lewis acid sites resulted from the extraframework Al species. Relatively, the peaks related to Cu species show less changes.

EPR was used to estimate the isolated Cu²⁺ amounts of the catalysts (Fig. S12, ESI†). In this study, the hydrated samples were used to avoid the formation of EPR silent species (e.g. Cu(OH)⁺) due to the dehydration treatment.¹⁶ The quantitative results are presented in Table S3 (ESI†). Both samples contain the same amounts of isolated Cu2+ ions (2.11 wt%), implying that most of the Cu species on the samples (86.8% of the total Cu loading) are active species for the NH3-SCR reaction. These results also demonstrate the good hydrothermal stability of isolated Cu²⁺ on the Na⁺-free Cu-SSZ-13.

Communication ChemComm

H₂-TPR experiments were used to evaluate the reducibility of Cu species. From Fig. S12 (ESI†), the fresh sample shows four reduction peaks, which are located at 203 (A), 364 (B), 495 (C) and 708 °C (D). According to the literature, 19 peaks A and B correspond to the reduction of isolated Cu²⁺ to Cu⁺. More specifically, the former peak may be associated with the reduction of [Cu(OH)]⁺-Z⁻ to Cu⁺, while the latter peak is due to the reduction of Cu²⁺-2Z⁻ to Cu⁺. Moreover, peak A may also contain the reduction of nanosized CuO particles to Cu⁰ (the CuO amount is low as deduced from EPR results). The small peak C arises from the reduction of Cu⁺ ions to Cu⁰, and the broad high-temperature peak D is assigned to the reduction of highly stable Cu⁺ to Cu⁰. ²⁰ As all the Cu⁺ species come from the reduction of Cu²⁺, the smaller peak area of (C + D) than that of (A + B) implies that some of the Cu⁺ species are difficult to reduce before 800 °C. After the hydrothermal treatment, the low-temperature peak moves forward, and the reduction of isolated Cu²⁺ species becomes easier, while the reduction of in situ formed Cu⁺ is more difficult. Given that the amount of isolated Cu²⁺ remains the same before and after aging, it is speculated that the location/distribution of Cu²⁺ species may alter during the hydrothermal aging and leads to the change of the reducibility of Cu species.

Based on the above characterizations, the variation of NH₃-SCR performance of the catalyst upon hydrothermal treatment can be analyzed as follows. It has been recognized that the NH3-SCR reaction follows a redox mechanism via a cycle of Cu²⁺and Cu⁺, ^{21,22} which means that the redox properties of the catalysts are critical to their SCR performance. Moreover, our work has evidenced that NH3 adsorbed on the moderate acid sites has higher reactivity for the low-temperature SCR reaction than on the strong acid sites. 23,24 Therefore, the enhanced lowtemperature NH3-SCR activity of the aged CuSSZ-13-4 catalyst should be attributed to its improved reducibility of Cu²⁺ to Cu⁺ and the increased moderate acid sites. On the other hand, the loss of strong Brønsted acid sites on the aged catalyst is unfavourable for the inhibition of the NH3 oxidation reaction, especially at high temperature, 20 which causes the apparent decrease in the high-temperature SCR activity.

In summary, an efficient one-pot synthesis strategy for Na⁺free SSZ-13 and Cu-SSZ-13 has been rationally developed. In this cooperative strategy, TMAdaOH has the most powerful effect in directing the formation of the CHA structure, the Cu-TEPA complex acts as a Cu source and as an OSDA, small size amine replaces NaOH to provide enough alkalinity for the gel system and reduce the usage of TMAdaOH, and the seeds help overcome the difficulty in nucleation and speed-up the crystallization. Thus, the syntheses can be accomplished with a rapid crystallization rate and high yield. The calcined Na⁺-free CuSSZ-13 possesses a high proportion of isolated Cu²⁺ ions and shows $\sim 100\%$ NO_x conversion in a wide temperature range of 200-450 °C in NH₃-SCR reaction under the investigated conditions. After hydrothermal treatment, the sample exhibits enhanced low-temperature activity (<200 °C), and the high-temperature activities can still be kept at > 80% at 550 °C. It is anticipated

that this methodology will benefit the syntheses of more Na⁺free zeolite catalysts.

This work was supported by the National Natural Science Foundation of China (21991090, 21991091) and Key Research Program of Frontier Sciences, Chinese Academy of Sciences (Grant No. QYZDB-SSW-JSC040) and DICP Funding (DICP ZZBS201807).

Conflicts of interest

There are no conflicts to declare.

References

- 1 H. Wang, L. Wang and F. S. Xiao, ACS Cent. Sci., 2020, 6, 1685-1697.
- 2 E. B. Clatworthy, S. V. Konnov, F. Dubray, N. Nesterenko, J.-P. Gilson and S. Mintova, Angew. Chem., Int. Ed., 2020, 59, 19414-19432.
- 3 D. K. Pappas, E. Borfecchia, M. Dyballa, I. A. Pankin, K. A. Lomachenko, A. Martini, M. Signorile, S. Teketel, B. Arstad, G. Berlier, C. Lamberti, S. Bordiga, U. Olsbye, K. P. Lillerud, S. Svelle and P. Beato, J. Am. Chem. Soc., 2017, 139, 14961-14975.
- 4 A. Koishybay and D. F. Shantz, J. Am. Chem. Soc., 2020, 142, 11962-11966.
- 5 C. Wen, L. Geng, L. Han, J. Wang, L. Chang, G. Feng, D. Kong and J. Liu, Phys. Chem. Chem. Phys., 2015, 17, 29586-29596.
- 6 D. Wang, L. Zhang, K. Kamasamudram and W. S. Epling, ACS Catal., 2013, 3, 871-881.
- 7 J. Wang, Z. Peng, Y. Chen, W. Bao, L. Chang and G. Feng, Chem. Eng. J., 2015, **263**, 9-19.
- 8 Z. Liu, T. Wakihara, K. Oshima, D. Nishioka, Y. Hotta, S. P. Elangovan, Y. Yanaba, T. Yoshikawa, W. Chaikittisilp, T. Matsuo, T. Takewaki and T. Okubo, Angew. Chem., Int. Ed., 2015, 54, 5683-5687.
- 9 Z. Liu, N. Nomura, D. Nishioka, Y. Hotta, T. Matsuo, K. Oshima, Y. Yanaba, T. Yoshikawa, K. Ohara, S. Kohara, T. Takewaki, T. Okubo and T. Wakihara, Chem. Commun., 2015, 51, 12567-12570.
- 10 J. Han, X. Jin, C. Song, Y. Bi, Q. Liu, C. Liu, N. Ji, X. Lu, D. Ma and Z. Li, Green Chem., 2020, 22, 219-229.
- 11 J. H. Kwak, R. G. Tonkyn, D. H. Kim, J. Szanyi and C. H. F. Peden, J. Catal., 2010, 275, 187-190.
- 12 D. Wang, F. Gao, C. Peden, J. Li, K. Kamasamudram and W. Epling, ChemCatChem, 2014, 6, 1579-1583.
- 13 L. M. Ren, L. F. Zhu, C. G. Yang, Y. M. Chen, Q. Sun, H. Y. Zhang, C. J. Li, F. Nawaz, X. J. Meng and F. S. Xiao, Chem. Commun., 2011, 47, 9789-9791.
- 14 R. Martinez-Franco, M. Moliner, J. R. Thogersen and A. Corma, ChemCatChem, 2013, 5, 3316-3323.
- 15 E. A. Eilertsen, B. Arstad, S. Svelle and K. P. Lillerud, Microporous Mesoporous Mater., 2012, 153, 94-99.
- 16 J. Song, Y. Wang, E. D. Walter, N. M. Washton, D. Mei, L. Kovarik, M. H. Engelhard, S. Prodinger, Y. Wang, C. H. F. Peden and F. Gao, ACS Catal., 2017, 7, 8214-8227.
- 17 L. Wang, W. Li, S. J. Schmieg and D. Weng, J. Catal., 2015, 324, 98-106.
- 18 R. Villamaina, S. Liu, I. Nova, E. Tronconi, M. P. Ruggeri, J. Collier, A. York and D. Thompsett, ACS Catal., 2019, 9, 8916-8927.
- 19 F. Gao, N. M. Washton, Y. Wang, M. Kollár, J. Szanyi and C. H. F. Peden, J. Catal., 2015, 331, 25-38.
- 20 L. Xie, F. Liu, L. Ren, X. Shi, F. S. Xiao and H. He, Environ. Sci. Technol., 2014, 48, 566-572.
- F. Gao, D. Mei, Y. Wang, J. Szanyi and C. H. F. Peden, J. Am. Chem. Soc., 2017, 139, 4935-4942.
- 22 C. Paolucci, A. A. Verma, S. A. Bates, V. F. Kispersky, J. T. Miller, R. Gounder, W. N. Delgass, F. H. Ribeiro and W. F. Schneider, Angew. Chem., Int. Ed., 2014, 53, 11828-11833.
- 23 X. Xiang, Y. Cao, L. Sun, P. Wu, L. Cao, S. Xu, P. Tian and Z. Liu, Appl. Catal., A, 2018, 551, 79–87.
- 24 Y. Cao, D. Fan, D. Zhu, L. Sun, L. Cao, P. Tian and Z. Liu, J. Catal., 2020, 391, 404-413.